Renewable Energy 138 (2019) 1–10

Contents lists available at ScienceDirect

Renewable Energy

journal homepage: www.elsevier.com/locate/renene

Energy conversion efficiency from low-head water to high-pressure gas☆

Yang Sun [a, d, *], Yuting Yao [a], Min Yan [b], Jiaming Liu [b], Haimiao Li [a], Yan Bao [c], Mingwei Lu [d]

[a] College of Harbour, Coastal and Offshore Engineering, Hohai University, Nanjing, China
[b] College of Water Conservancy and Hydropower Engineering, Hohai University, Nanjing, China
[c] State Key Laboratory of Hydrology-water Resources and Hydraulic Engineering, Nanjing Hydraulic Research Institute, Nanjing, China
[d] Miao Hui Energy Technology Co. Ltd., Shanghai, China

ARTICLE INFO

Article history:
Received 28 February 2018
Received in revised form
12 November 2018
Accepted 15 January 2019
Available online 21 January 2019

Keywords:
Two-phase gas-liquid flow
Gas-water energy conversion efficiency
Low-water-head hydropower

ABSTRACT

Low-water-head hydropower is usually viewed as useless because of its inefficiency. The Low-Water-Head Hydropower Project can automatically transmute low-water-head hydropower into high-pressure gas power, which will solve the problem of the under-utilization of low-water-head hydropower. Considering the under-utilization of low-water-head hydropower because of its inefficiency, we propose a less intrusive and more efficient solution: the Low-Water-Head Hydropower Project with an automatic pump, which can transmute the low-water-head hydropower into high-pressure gas power. The energy-transfer process from water to air has not been investigated in previous studies. The goal of this study is to improve the energy conversion efficiency of the project. The goal of our study is to improve the energy conversion efficiency. The energy-transfer process from water to air has not been a focus in previous studies. Hence, a full-scale experiment was conducted, and the formula for the energy conversion efficiency η was deduced. Energy balance equations based on the one-dimensional homogeneous model from the Bernoulli equation were established. Through the energy balance equation, the percentages of energy loss of different forms were determined. Wider and higher outlet pipes have higher η values. From an engineering perspective, the frictional head loss in all cases is so small that the frictional head loss caused by sidewall friction can be neglected. The change in temperature does not practically affect the sidewall friction effect. These conclusions can be applied in engineering applications.

1. Introduction

The Chinese remote mountainous region is rich in water resources. However, the water available for drinking and irrigation is lacking in these regions because the river flows at the foot of the mountains and large areas of farmland are located on the hillside, as shown in Fig. 1. Wang and Li [1] noted that, data provided by the water authority of Menglian County indicates that there are 13431 villages in Yunnan Province. Depending on data provided by the water authority of Menglian County, there are 13431 villages in Yunnan Province. There is a lack of water supply in approximately 40% of these villages. Similar situations occur in Jiangxi Province, Sichuan Province and Guizhou Province.

In addition, scattered villages and the instable voltage of the power grid across the region drastically increase the total cost of delivering water to villagers using traditional pumping. Water power is probably the most-used form of energy given by nature. Water-power electricity generation is low cost, but the dropping variance in congenital rivers must be large. The problem of making full use of the hydropower of low water-head rivers at the foot of mountains is an urgent livelihood issue. To utilize low water-head rivers, the design of energy conversion equipment is a key technology. Considering the problem of the under-utilization of low-head water power because of its inefficiency, a less intrusive and more efficient solution is proposed: the Low-Water-Head Hydropower Project with an automatic pump, which can transmute low-water-head hydropower into high-pressure gas power and is highly efficient.

Renewable energy has significant limitations in terms of stable

☆ This document is a collaborative effort.

* Corresponding author. College of Harbour, Coastal and Offshore Engineering, Hohai University, Nanjing, China.
E-mail address: sunyang_hhu@hhu.edu.cn (Y. Sun).

https://doi.org/10.1016/j.renene.2019.01.062
0960-1481/

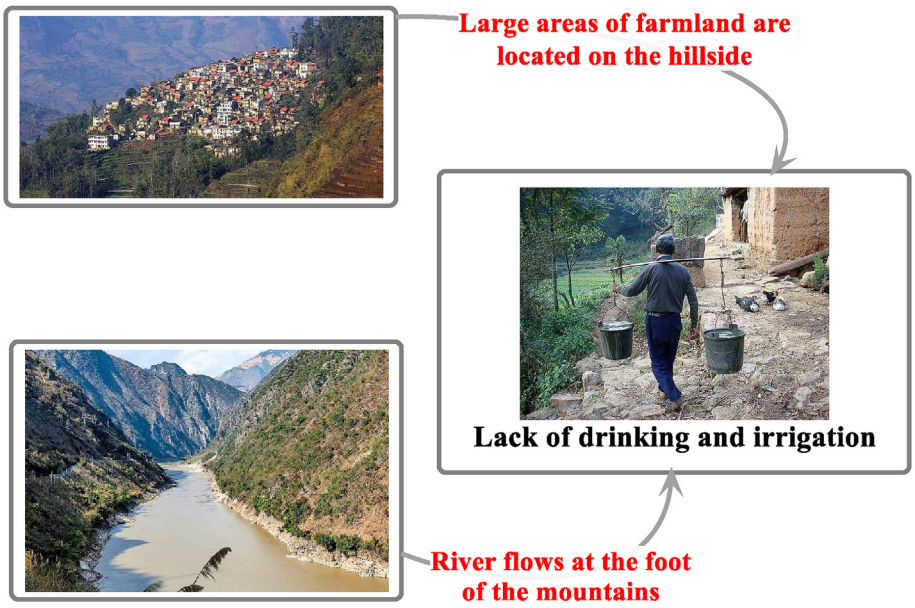

Fig. 1. The water supply status in the Chinese remote mountainous region.

power generation and integration with the public power grid. Turbine technology can minimize energy loss and aid in controlling the power. Using turbine technology, a series of studies by Liu and Tan [2], Hao and Tan [3] and Thapa et al. [4] on renewable energy were conducted. Researchers (e.g., Francois et al. [5], Mankbadi and Mikhail [6], Date et al. [7], Parygin et al. [8]) planned to use the turbine to produce energy from low-water-head hydropower, which required high labor costs and maintenance costs. Our approach to using low-water-head source is different from previous approaches. The Low-Water-Head Hydropower Project can pump water up to hundreds of meters high under the condition that the drop in the river is 2–10 m, and it does not have to be connected to the grid or require management when built. Similar research by Roberts A [9] showed that no greenhouse gas emissions were produced during operation and that the system was cheap to run and was capable of operating passively for prolonged periods. They harnessed the water hammer effect and substituted the pressurized water delivery system with an energy conversion mechanism. However, the time-averaged efficiency varied from 0.3 to 1.7%, which is far less than the 14–44% of this article.

The Low-Water-Head Hydropower Project consists of two parts: the Gas-Water Energy Conversion Equipment (Fig. 3), and the High-Pressure Pumps. The first part turns natural air into high-pressure gas using the drop of the river, and the second part pumps water up to tens or hundreds of meters high using the high-pressure gas. High-Pressure Pumps have received considerable attention from researchers (e.g., Zenz [10], Gvirtzman and Gorelick [11], Francois et al. [5], Guet and Ooms [12]) in the last three decades. The Gas-Water Energy Conversion Equipment is also a focus of research and is considered in this paper.

The goal of the study is to improve the energy conversion efficiency from low-head water to high-pressure gas. Understanding the possible mechanisms of the energy-transfer process is a key step. The energy-transfer process from water to air has not been thoroughly examined in previous studies. However, numerous studies of the gas-liquid two-phase flow pressure drop have been conducted, which aid in understanding the quantitative estimation of the energy-transfer process. Extensive theoretical and experimental studies have been conducted to calculate the two-phase pressure drop. Researchers such as Lockhart and Martinelli [13], Dukler et al. [14], Beattie and Whalley [15], Mullersteinhagen and Heck [16], Triplett et al. [17], Sawai et al. [18] and Shannak [19] use the effective formulation method, which predicts the two-phase frictional pressure drop. Many theoretical and experimental studies have also been conducted using various forms of pipes to observe the effects. Zhao and Bi [20] examined the pressure drop characteristics of the gas-liquid two-phase flow in vertical miniature triangular channels. Based on the mass and energy balance and experimental results, Nilpueng and Wongwises [21] developed a new empirical correlation to calculate the two-phase pressure drop in vertical, internally wavy 90-degree bends. Gas-liquid two-phase phenomena in capillary tubes were investigated by Fukano and Kariyasaki [22], with special attention on the flow patterns, time-varying void fraction and pressure loss. These articles introduced concepts to help understand the energy loss generated by low-head water and how to calculate it.

In the mixing process of gas and liquid, there may be large energy loss because of the momentum transfer between gas and liquid. However, the momentum transfer was commonly neglected when evaluating the pressure drop in earlier articles, where there is no violent two-phase mix. Based on the method in two-phase flow studies to detect a pressure drop, a new method is proposed to estimate the energy loss of different forms generated by the low-head water and focuses on the vertical downflow, where the gas and liquid dramatically mix. The momentum transfer between air and water is also considered. As a result, energy balance equations can be established. Using the energy balance equation, the percentages of the energy loss of different forms are determined. In addition, a rough estimate of the percentage of gas-liquid mixing energy loss caused by the momentum transfer is obtained. Then, based on the experimental data, the effects of the outlet pipe on the energy conversion efficiency are analyzed. Fig. 2 has carried on an introduction to the research line.

2. Experimental setup and procedure

The Gas-Water Energy Conversion Equipment is shown in Fig. 4 and the model test equipment is shown in Fig. 5. It is comprised of three main sections: the vertical downcomer, the horizontal gas-liquid primary separator and the water outlet pipe.

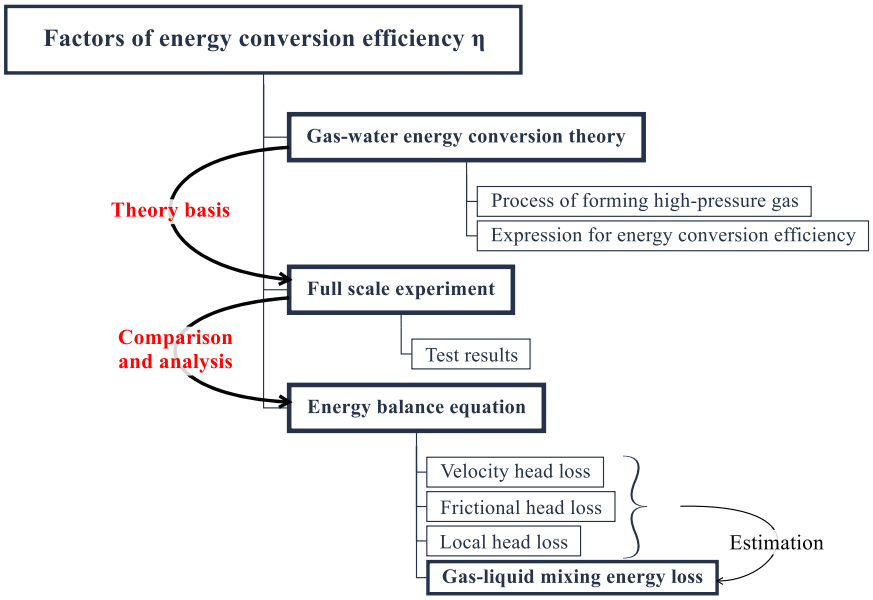

Fig. 2. Research line.

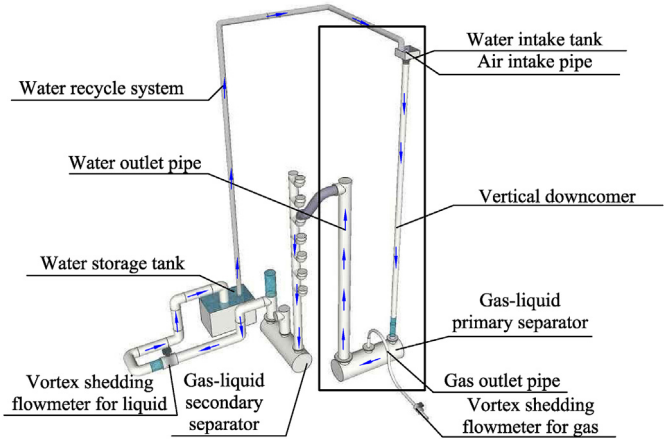

Fig. 3. Schematic diagram of the experimental system. Details of the segment in the box are shown in Fig. 4.

In the first section, the low-head water normally drains to the vertical downcomer by gravity. When water particles separate from one another, a negative pressure is generated. Air is drawn into the vertical down flow pipe because of the negative pressure. After dropping a long distance along the vertical pipe, the unit air mass is subject to an increase in pressure from the two-phase flow column above it, and the usable high-pressure gas ultimately appears at the end of the pipe.

When the two-phase flow passes through a dividing junction (on top of our second section, which is the gas-liquid primary separator in Fig. 4), an uneven distribution of the gas and liquid phases commonly appears between the outlets. This phenomenon is called phase separation [23]. The phase split of the gas-liquid two-phase flow through small holes at the pipe wall was experimentally investigated by Liang et al. [24]. Their experimental results show that the phase-splitting behavior is significantly affected by the number and position of the sampling holes and superficial velocities of the gas and liquid. These experiments consisted of an identical number and position of holes with different superficial velocities of the gas and liquid. The water velocity is controlled by a high-powered pump in the water storage tank to pump water up to the water intake tank to simulate the drop of the river in nature. The test was performed under the condition that the liquid volumetric flow rate was sufficiently large to submerge the vertical downcomer and form a closed space. Gas will escape from the water if the water volume is small, in which case the study of the energy conversion efficiency η is meaningless.

A full-scale experiment was conducted, as shown in Fig. 4, and the test duration was approximately one year. The tests were conducted at room temperature and atmospheric pressure in a semi-enclosed environment. The temperature was 0–30 °C in the lab regardless of when it was measured. After the equipment is activated, water flows into the vertical downcomer from the water intake tank and air is spontaneously mixed into the water. The gas phase is compressed into a high-pressure gas and separated from the liquid phase in the gas-liquid separator, where the gas phase passes through the gas outlet pipe and the liquid phase passes through the water outlet pipe. The height of the outlet pipe is consistent with the relative pressure of high-pressure gas using the isobaric surface analysis method (Fig. 4), so that the pressure of high-pressure gas can be derived from the height of the outlet pipe. The vortex-shedding flowmeter installed at the end of the gas outlet pipe was used to measure the gas volumetric flow rate at room temperature and atmospheric pressure. We used another vortex shedding flowmeter to measure the liquid volumetric flow rate. Even if a two-phase flow has been separated, the air in the water cannot be completely separated; thus, it may affect the accuracy of the vortex shedding flowmeter for the liquid. Therefore, by applying another separator, the residual air in the water is eliminated. Finally, all water is gathered into a water storage tank to enable efficient water recycling. The formation mechanism of the high-pressure gas is described in section 3.

Intelligent vortex shedding flowmeters are mainly used to measure the flow in pipelines of various media, such as gas, liquid and steam. It is characterized by a small pressure loss, high measure

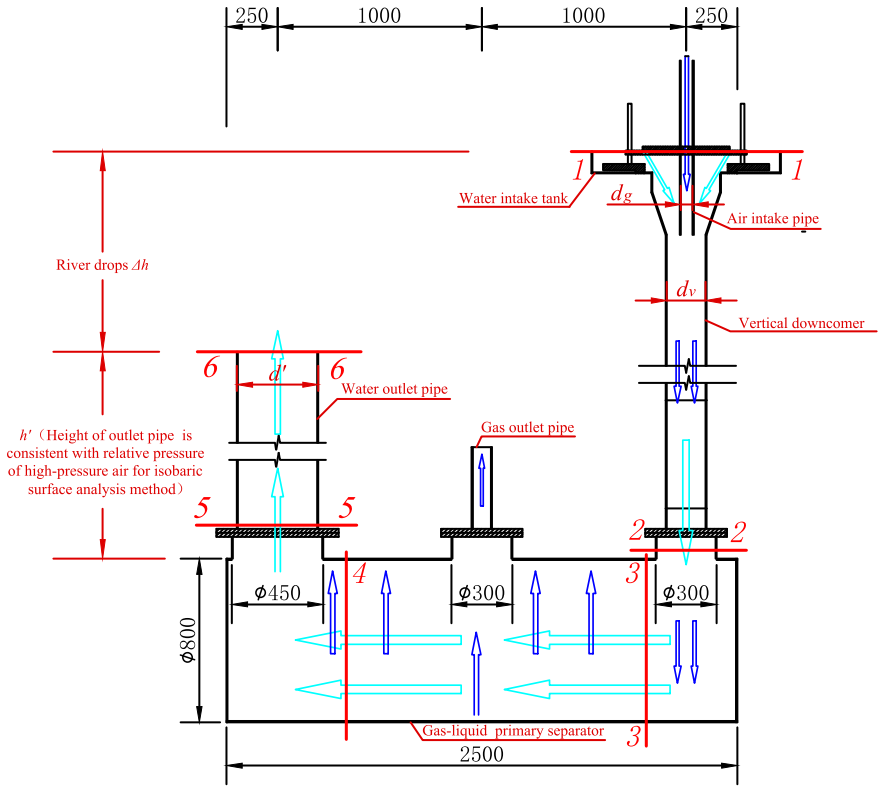

Fig. 4. Size of the Gas-Water Energy Conversion Equipment and layout of the sections. (unit: mm).

Fig. 5. Experimental setup.

range and high precision. The measurement of the volumetric flow rate is almost free from the influence of pressure, fluid density, viscosity, temperature and other parameters. Therefore, the intelligent vortex shedding flowmeter has high reliability, low maintenance and stable operation. It can fully meet our requirements in the semi-closed environment for a long time, for highly consistent test data in different batches. Intelligent vortex shedding flowmeters use a piezoelectric stress sensor. They can work effectively in the temperature range of −20 °C - +450 °C. In addition, the water circulation system uses a special water supply inverter with 18.5 kW of power. The volumetric flow rate of the liquid is controlled by the high-power pump in the water storage tank, which pumps water into the upper water intake tank and maintains a certain elevation difference (2 m – 6 m) between the water intake tank and the top of the outlet pipe to simulate the river drop in nature.

The gas-liquid separator is made of ordinary steel and is designed to endure the unbalanced power resulting from the pressure differential. The parts of the separator must be welded together, so it is watertight and airtight. The horizontal cylinder in the lower part has three round holes every meter to build connections with the vertical downcomer, gas outlet pipe and water outlet pipe (Fig. 4). The materials and sizes of the other components of the equipment are listed in Table 1, in which polyvinyl chloride (PVC) and polyethylene (PE) are used.

Table 1
Materials of the gas-water energy conversion equipment.

Portions of the Equipment	Materials	Size of Unit (mm)
Water intake tank	Fe360A	2000 × 800 × 500
Air intake pipe	PVC hard pipe	Φ25, Φ32, Φ40, Φ50, Φ75, Φ110
Vertical downcomer	PVC hard pipe	Φ160, Φ200, Φ250
Gas-liquid separator	Fe360A	Φ25, Φ32, Φ40, Φ50, Φ75, Φ110
Gas outlet pipe	PE corrugated pipe	Φ10
Water outlet pipe	PVC hard pipe	Φ400
Water storage tank	Fe360A	
Water recycle system	PE corrugated pipe	

3. Gas-water energy conversion theory

3.1. Process of forming high-pressure gas

Approaching the gas-water energy conversion theory as a two-phase flow problem, for the vertical downcomer, when the flow rate of water is sufficiently large, the upside of the pipe forms a liquid seal.

The water particle movement of the horizontal pipe flow is different from that of a vertical pipe flow. In the horizontal pipe, all water particles have identical flow velocities and have no tendency to break because there is no acceleration along the pipe line. In contrast, in the vertical pipe, all water particles are subject to the force of gravity. Each water body at different locations of the vertical pipe has a different flow velocity. The lower pipe has a higher flow velocity. The water bodies separate from each other vertically, and the separative trend is increasingly more distinct when the distance of flow increases. When the water bodies separate from one another, a negative pressure is generated. There is a general tendency that the filled flow enters in the interval between the breakage of the main flow till the balance of pressure between the two parts is achieved.

The portion at the entrance of the variational diameter pipe is shown in Fig. 4. There is a gas phase above the portion and a gas-liquid phase below it (Fig. 4). In comparison, there is a gas-liquid phase in both the upper and lower sections of the pipe. When the equipment turns on, a non-uniform stern flow is observed in the vertical downcomer. Notably, a uniform two-phase flow of the vertical pipe forms and continues to vertically drop. After dropping a long distance along the vertical pipe, the unit air mass is subjected to increasing pressure from the two-phase flow column above it and high-pressure gas forms.

3.2. Expression for the energy conversion efficiency

The energy efficiency η is the ratio of the usable energy output of an energy conversion equipment to the energy input. Energy conversion efficiency is defined differently for different needs. Researchers (e.g., Zhao et al. [25], Roberts A [9], Li et al. [26]) have proposed different formulas based on where their energy came from and how the work was done. There is no consistent or well-accepted definition of the energy conversion efficiency η between water power and high-pressure gas power. The energy conversion efficiency η can be predicted by:

$$\eta = \frac{E_{gas}}{E_{liquid}} \tag{1}$$

where E_{gas} and E_{liquid} are the water power and high-pressure gas power, respectively.

The water power in Eq. (1) is given by:

$$E_{liquid} = mg\Delta h \tag{2}$$

where, m is the mass of low head water, g is the local acceleration of gravity and Δh is the river drops.

The high-pressure gas power in Eq. (1) is:

$$E_{gas} = \int_{V_1}^{V_2} PdV = \int_{V_1}^{V_2} \frac{V_1P_1}{V}dV = V_1P_1 \ln\frac{P_1}{P_2} \tag{3}$$

where P_2 is the pressure at the trial sites, V_2 is the gas volume under pressure at the trial sites, P_1 is the pressure of the high-pressure gas, and V_1 is the gas volume under high pressure.

The low-water-head hydropower E_{liquid} is converted to high-pressure gas power E_{gas}. High-pressure gas can do work when it expands at room temperature and atmospheric pressure until the pressure of this high-pressure gas gradually decreases to one bar.

Therefore, the energy conversion efficiency η can be predicted by:

$$\eta = \frac{V_1P_1 \ln\frac{V_2}{V_1}}{mg\Delta h} \tag{4}$$

$$V_1P_1 = V_2P_2 \tag{5}$$

From Eq. (5), Eq. (6) can be derived:

$$\eta = \frac{V_1P_1 \ln\frac{P_1}{P_2}}{mg\Delta h} = \frac{V_2P_2 \ln\frac{P_1}{P_2}}{mg\Delta h}$$

By measuring Q_g and Q_l at atmospheric pressure P_0, η is calculated as follows:

$$\eta = \frac{E_{gas}}{E_{liquid}} = \frac{Q_gP_0 \ln\frac{P_0+\Delta P}{P_0}}{Q_l\rho_l g\Delta h} \tag{6}$$

where Q_g is the gas volumetric flow rate, Q_l is the liquid volumetric flow rate, ρ_l is the density of the liquid phase, and ΔP is the relative pressure of the high-pressure gas.

Based on the formula structure analysis of Eq. (6), P_0, ρ_l and g are roughly constant, and η is under the direct effect of Q_g, Q_l, ΔP and Δh. Q_g, Q_l, ΔP and Δh are obtained from direct measurements and η is calculated using Eq. (6).

4. Analysis of test results

4.1. Effect of the outlet pipe diameter

Two series of comparison experiments were designed to study the effect of d' on η. The experiments used Φ110 and Φ250 outlet pipes. The data processing results were consolidated into 3-

dimensional surface images, as shown in Fig. 6.

The results shown in Fig. 6 indicate that when the remaining conditions are completely identical, η for $d' = 250$ mm is always greater than η for $d' = 110$ mm. Thus, a wider outlet pipe has a higher η. Therefore, for the energy conversion efficiency, a large diameter outlet pipe is often preferred. The theoretical analysis is explained in detail in section 5.2.

4.2. Effect of the outlet pipe height

Forty-two sets of experimental data using the Φ160 vertical downcomer were consolidated into 3-dimensional surface images, as shown in Fig. 7 (a). Seventy-three sets of experimental data using the Φ200 vertical downcomer were consolidated into 3-dimensional surface images, as shown in Fig. 7 (b).

In Fig. 7, when the remaining conditions are completely identical, η of $h' = 6$ m is always greater than η of $h' = 5$ m. Thus, a higher outlet pipe has a higher η. Therefore, we propose that a higher outlet pipe is better suited for engineering applications to improve the energy conversion efficiency. Because the outlet pipe is buried underground in engineering, if the outlet pipe is higher, it is buried at a greater depth and the costs will increase. Thus, the selected value of h' must be carefully analyzed before use in engineering applications.

Here, we theoretically analyze the causes of the effect of the outlet pipe height. There is a direct relationship between h' and ΔP. ΔP increases with h', and other variables in Eq. (6) are almost constant with changing h'. Thus, a higher outlet pipe has a larger η. According to the statistical analysis of the test data shown in Figs. 6 and 7, the energy conversion efficiency is 14–44%.

5. Theoretical estimation of energy loss

5.1. Energy balance equation

In the gravitational field, with identical total heads, a uniform uncompressed ideal steady fluid flows through cross-sections 1 and 6 (Fig. 4). Since the flow in the experimental system satisfied the prerequisite of conservation of mechanical energy, the Bernoulli equation derived from the conservation of mechanical energy can be used to model the calculation. This calculation model is only applicable for a rough estimation of different energy loss forms to meet the requirements of engineering design. A gas-liquid two-phase flow equation through cross-sections 1 and 6 is deduced based on the one-dimensional homogeneous model from the Bernoulli equation:

$$z_1 + \frac{P_1}{\rho_1 g} + \frac{u_1^2}{2g} = z_6 + \frac{P_6}{\rho_6 g} + \frac{u_6^2}{2g} + h_{1-2} + h_{2-3} + h_{3-4} + h_{4-5} + h_{5-6} \tag{7}$$

where u is the homogeneous fluid flow speed at a point on a streamline, g is the acceleration due to gravity, z is the elevation of the point above a reference plane, P is the pressure at the selected point, and ρ is the density of the fluid at all points in the fluid. As shown in Fig. 4, cross-section 1 is in the upper part of the vertical downcomer, cross-section 2 is in the lower part of the vertical downcomer, cross-section 3 is at the entrance of the gas-liquid primary separator, cross-section 4 is at the exit of the gas-liquid primary separator, cross-section 5 is in the lower part of the outlet pipe and cross-section 6 is in the upper part of the outlet pipe. h_{1-2}, h_{2-3}, h_{3-4}, h_{4-5} and h_{5-6} are the head losses of different sections. h_{1-2}, h_{3-4} and h_{5-6} basically consist of the frictional head loss and h_{2-3} and h_{4-5} basically consist of the local head loss.

$z_1 = \Delta h + h'$, $z_2 = h'$, and $u_1 = 0$ are obtained from the relative positions of incoming and outgoing flow (Fig. 4). $P_1 = 0$ and $P_6 = 0$ are derived based on the normal pressure and room temperature. By replacing z_1, z_2, u_1, P_1 and P_6 in Eq. (7), Eq. (7) is obtained:

$$\Delta h = h_v + h_{1-6} \tag{8}$$

$$h_v = \frac{u_6^2}{2g} \tag{9}$$

where h_{1-6} is the sum of the head losses between cross-sections 1 and 6:

$$h_{1-6} = h_{frc} + h_{loc} + h_{mix} \tag{10}$$

Corresponding to the parameters in Fig. 8, h_{frc}, h_{loc} and h_{mix} are the frictional head loss, local head loss and gas-liquid mixing energy loss, respectively. h_v in Eq. (8) is the velocity head.

PVC pipes are widely used in studies because of their convenience and simplicity in modeling and testing. The PVC pipes and fitting in walls are uniform and smooth, and the flow resistance is small. In some engineering applications, other durable materials are used to prolong the operational lifetime and adapt to different environments. Therefore, study of the frictional head loss provides valuable guidance. The energy-transfer process from water to air has not been thoroughly examined in previous studies. However, numerous studies of the gas-liquid two-phase flow pressure drop have been conducted. The pressure drop in a straight pipe can be expressed in terms of the frictional pressure drop, gravity pressure drop and accelerated pressure drop. To calculate the two-phase pressure drop, extensive theoretical and experimental studies have been conducted. Measurements of two-phase pressure drops contain a great dispersion of plus or minus 20% because it is difficult to accurately evaluate. There are pipe fittings such as bend pipes and reducing joints in the equipment, where the fluid disturbance is dramatically increased over that of a single-phase flow. Thus, to analyze the frictional effect at the pipe wall, the formula is used to calculate the frictional pressure drop including the local frictional

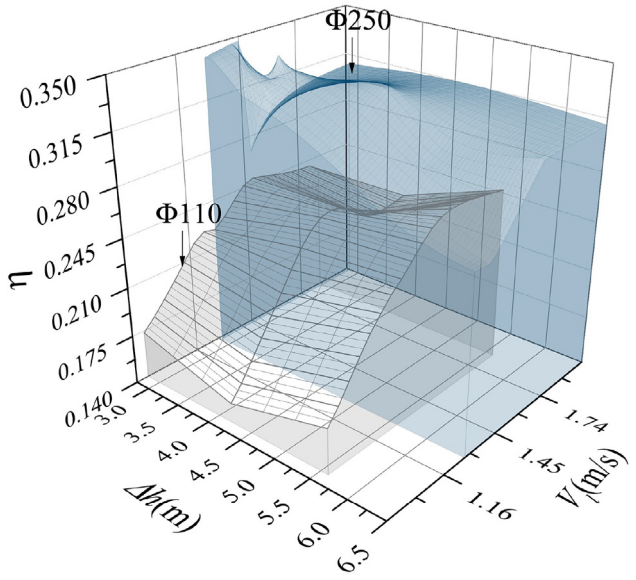

Fig. 6. Effect of d' on η. d' is the diameter of outlet pipe, h' is the height of outlet pipe and η is the energy conversion efficiency.

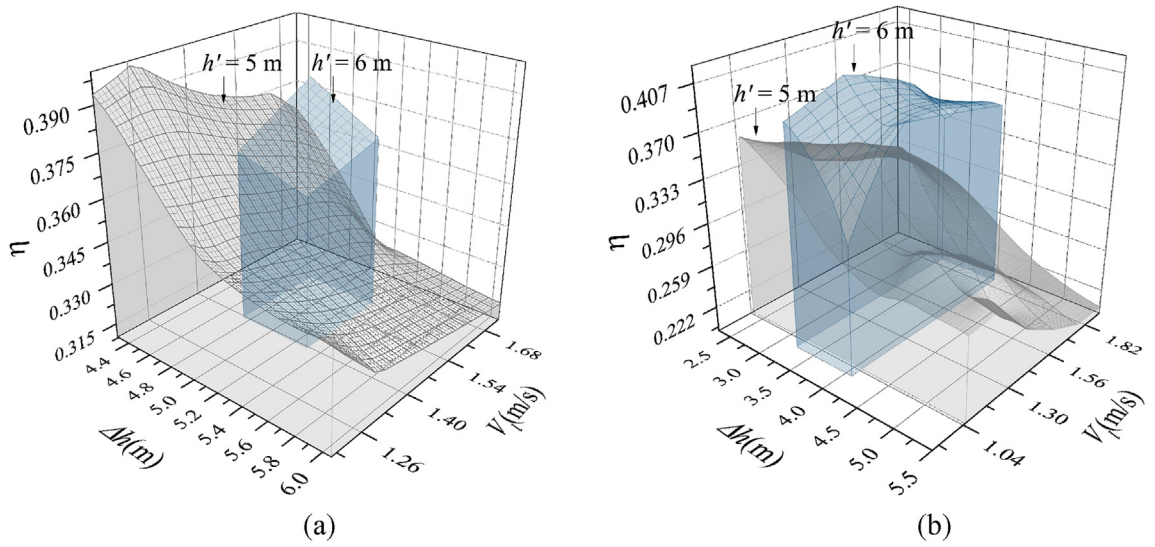

Fig. 7. Effect of h' on η. d' is the diameter of outlet pipe, h' is the height of outlet pipe and η is the energy conversion efficiency.

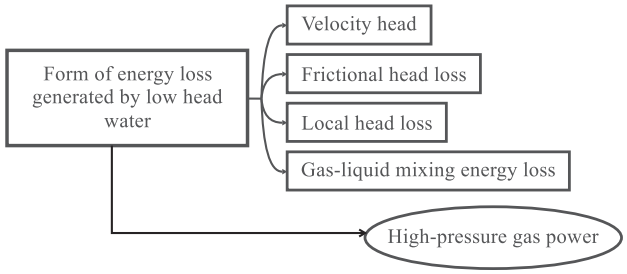

Fig. 8. Form of energy loss generated by the low head water.

pressure drop.

To calculate the frictional pressure drop in the segment between cross-sections 1 and 2 and the segment between cross-sections 3 and 4, the Chisholm formula [27] is typically used. To calculate the frictional pressure drop in the segment between cross-sections 5 and 6, the equation of the single-phase flow for friction loss along the pipe is used. The conversion method is used to calculate the local frictional pressure drop in the segments between cross-sections 2 and 3 and cross-sections 4 and 5. There is an assumption that the local frictional pressure drop accounts for approximately 10% of the sum of the frictional pressure drops of the three segments.

As a result, the head loss caused by friction at the wall is calculated in different operating conditions.

5.2. Estimation of the velocity head

Based on Eq. (8), part of the total energy loss is in the form of the velocity head in cross-section 6 and the other part is in the form of energy loss between cross-sections 1 and 6. This relationship is shown in Fig. 8. The flow in cross-section 6 is merely a single-phase liquid flow. Therefore, it is easy to derive estimates of the velocity head h_v in cross-section 6.

One set of data is from the condition of the Φ110 vertical down-flow pipe and Φ110 outlet pipe; the other set of data is from the condition of the Φ110 vertical down-flow pipe and Φ250 outlet pipe. The Q_l of the two sets is 40 m^3/h to 70 m^3/h. According to 212 groups of testing data, the values of velocity head can be calculated and the measured variables in the test were Q_l and d. Then, the effect of the outlet pipe diameter on the velocity head ratio can be estimated using Eq. (9), as shown in Fig. 9, where u_6 is given by

$$u_6 = \frac{4\pi Q_l}{d'^2} \tag{11}$$

To enhance the application value of estimation, working conditions are assumed as the different diameters of outlet pipes ($d' = 110 - 500$ mm), with multiple altitudes of river drops ($\Delta h = 2 - 7$ m) and a wide range of river flow rates ($Q_l = 40 - 70\ m^3/h$). Then, the ratios of the velocity head in these cases are estimated. The results of the estimations are summarized in Fig. 10.

As shown in Fig. 9, when PVC pipes with a small Φ110 diameter are used, the ratio of the velocity head is approximately 1 – 7 %, too large to be neglected from an engineering viewpoint. In contrast, the ratio of 0.04 – 0.16 % when PVC pipes with large diameter Φ250 are used is so small that it is negligible. Thus, if d' is further reduced, the ratio of the velocity head can remarkably increase. Conversely, if d' increases, the ratio of the velocity head will

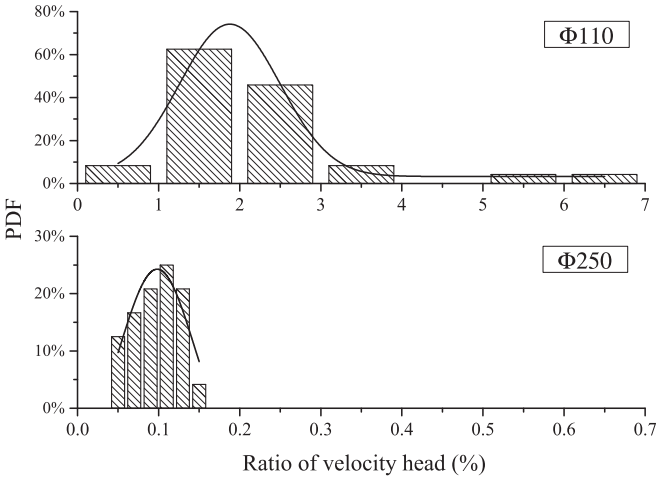

Fig. 9. Comparison of the fitted distributions (solid lines) and experimental observations (histograms) for water outlet pipes of different diameters. PDF is the abbreviation for probability density function.

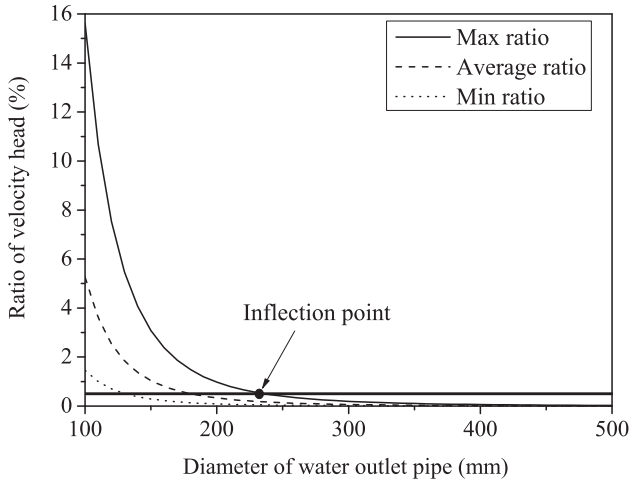

Fig. 10. Simulated curves of the velocity head ratio using water outlet pipes for Φ100 and Φ500.

decrease.

The theoretical estimates correspond with the test results in section 4.1. However, there are slight differences between the theoretical and experimental results. In the experiments, the difference in η between the Φ110 pipe and the Φ250 pipe is 10% (Fig. 6), which is much higher than the theoretical 7% (Fig. 9). Thus, the practical effect of d' is greater than the theoretical effect due to some uncertainties.

As shown in Fig. 10, when d' is 100–500 mm, the ratio of the velocity head decreases with the increase in d' and approaches zero. For the current situation in which the test results are slightly larger than the estimated theoretical results, there is an assumption that the velocity head ratio of 0.5% is sufficiently small to be considered negligible. Thus, to eliminate the effect of the velocity head in the actual project, inflection points on the simulated curves of velocity head ratio must be found and summarized into tabular results (Table 2), where the ratio is 0.5%. Accordingly, engineers can follow Table 2 to determine d' based on the specific flow rate and river drops in actual projects.

5.3. Estimation of the frictional head loss of the two-phase flow segment

In calculating the frictional pressure drop in the segment between cross-sections 1 and 2 and the segment between cross-sections 3 and 4, the Chisholm formula [27] is typically used.

The Reynolds numbers of the liquid phase and gas phase are given by Eqs. (12) and (13), respectively.

$$Re_l = \frac{(1-x)Gd}{\mu_l} \tag{12}$$

Table 2
Selection of diameter of outlet pipe.

Flow rate of river (m^3/h)	River drops (m)					
	2 – 3	3 – 4	4 – 5	5 – 6	6 – 7	7 – 8
≤ 100	≥ 290	≥ 260	≥ 240	≥ 230	≥ 220	≥ 210
100 – 150	≥ 350	≥ 320	≥ 300	≥ 280	≥ 270	≥ 260
150 – 200	≥ 400	≥ 370	≥ 340	≥ 320	≥ 310	≥ 300
200 – 250	≥ 450	≥ 410	≥ 380	≥ 360	≥ 340	≥ 330
250 – 300	≥ 490	≥ 450	≥ 420	≥ 390	≥ 380	≥ 360

$$Re_g = \frac{xGd}{\mu_g} \tag{13}$$

where G is the mass velocity, d is the tube diameter, x is the dryness fraction, and μ_l and μ_g are the absolute viscosities of liquid and gas, respectively.

The environmental temperature of the device is approximately 0–30 °C, so Re_l and Re_g are calculated at the environmental temperatures of 0 °C and 30 °C. When the temperature is 0 °C, μ_l is 1.789×10^{-5} N·S/m^2 and μ_g is 1.716×10^{-5} N·S/m^2. When the temperature is 30 °C, μ_l is 8.017×10^{-4} N·S/m^2 and μ_g is 1.863×10^{-5} N·S/m^2. According to Eqs. (12) and (13), $Re_l > 1000$ and $Re_g < 1000$ for 212 groups of testing data, as shown in Figs. 11 and 12. Then, the value of c in Eqs. (19) and (20) is 10 according to the factors recommended by Chisholm.

The friction pressure drop gradient of the liquid phase and gas phase are estimated by:

$$\left(\frac{dp_l}{dz}\right)_l = \frac{\lambda_l}{d}\frac{G^2}{2}(1-x)^2 v_l \tag{14}$$

$$\left(\frac{dp_l}{dz}\right)_g = \frac{\lambda_g}{d}\frac{G^2}{2}(x)^2 v_g \tag{15}$$

The liquid phase flow is turbulent flow, so the liquid phase friction factor λ_l is:

$$\lambda_l = 0.3164 Re_l^{-0.25} \tag{16}$$

The gas phase flow is a laminar flow, so the gas phase friction factor λ_g is:

$$\lambda_g = \frac{64}{Re_g} \tag{17}$$

where v_l is the specific volume of liquid, and v_g is the specific volume of gas. When the temperature is 0 °C, v_l is 1/999.9 m^3/kg, and v_g is 1/1.293 m^3/kg. When the temperature is 30 °C, v_l is 1/995.7 m^3/kg, and v_g is 1/1.165 m^3/kg.

The Lockhart-Martinelli parameter X is given by:

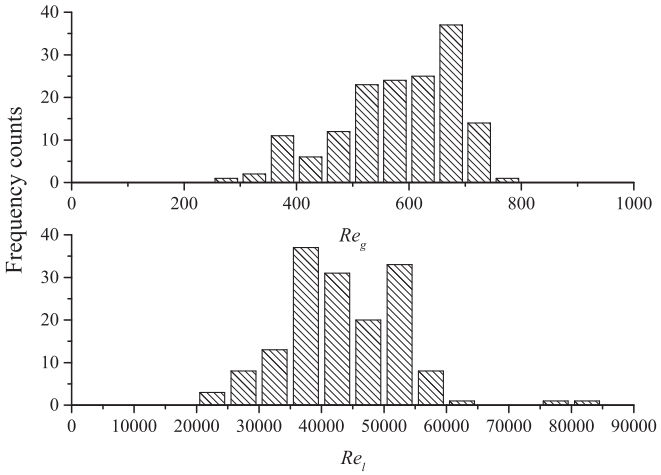

Fig. 11. The Reynolds numbers of the liquid phase and gas phase in the temperature of 0 °C.

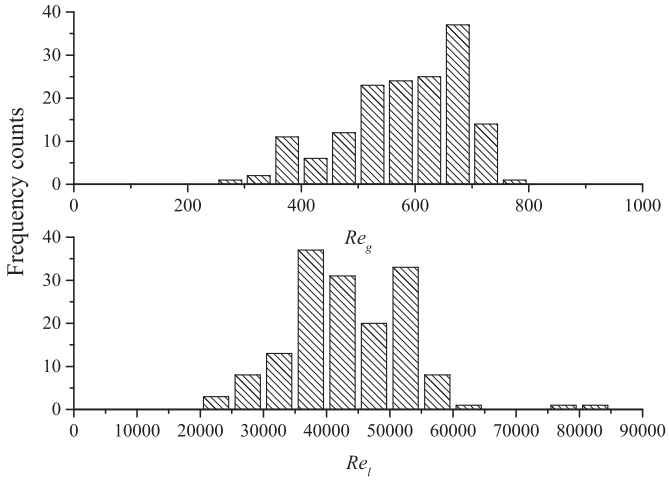

Fig. 12. The Reynolds numbers of the liquid phase and gas phase in the temperature of 30 °C.

$$X^2 = \frac{\left(\frac{dp_l}{dz}\right)_l}{\left(\frac{dp_l}{dz}\right)_g} \tag{18}$$

The conversion coefficients of the liquid phase and gas phase are as follows:

$$\Phi_l^2 = 1 + \frac{c}{X} + \frac{1}{X^2} \tag{19}$$

$$\Phi_g^2 = 1 + cX + X^2 \tag{20}$$

The frictional pressure drop gradients of the two-phase flow are:

$$\frac{dp_t}{dz} = \Phi_g^2 \left(\frac{dp_t}{dz}\right)_g \tag{21}$$

$$\frac{dp_t}{dz} = \Phi_l^2 \left(\frac{dp_t}{dz}\right)_l \tag{22}$$

Ultimately, the frictional head loss is given by:

$$h_f = \frac{\frac{dp_l}{dz} L}{\rho g} \tag{23}$$

5.4. Estimation of the frictional head loss of the single-phase flow segment

To calculate the frictional pressure drop in the segment between cross-sections 5 and 6, we use the single-phase flow equation for friction loss along the pipe.

This section introduces a commonly used empirical formula for the single-phase flow for friction loss along the pipe and applies it to calculation of the frictional pressure drop in the segment between cross-sections 5 and 6.

$$h_f = \frac{fLQ^m}{d^b} \tag{24}$$

where L is the length of the pipe, Q is the flow rate, d is the diameter of the pipe, and f, m and b are empirical values. A reference table (Table 3) is provided as a guide for using PVC, aluminum alloy, asbestos cement, new steel, old steel and reinforced concrete (RC).

Table 3
Detailed parameters table of f, m and b.

Materials of pipes	f	m	b
PVC	0.948×10^5	1.77	4.77
Aluminum alloy	0.861×10^5	1.74	4.77
Asbestos cement	1.455×10^5	1.85	4.89
New steel	5.65×10^5	1.85	5.04
Old steel	6.25×10^5	1.90	5.10
RC ($n = 0.013$)	1.312×10^6	2.00	5.33
RC ($n = 0.014$)	1.516×10^6	2.00	5.33
RC ($n = 0.015$)	1.749×10^6	2.00	5.33
RC ($n = 0.017$)	2.24×10^6	2.00	5.33

The pipes in our tests are PVC pipes; therefore, f is 0.948×10^5, m is 1.77, and b is 4.77. Based on the parameters of f, m and b in Table 3 and the experimental data, the frictional head loss in the segment between cross-sections 5 and 6 can be estimated when reinforced-concrete pipes are used.

5.5. Estimation of the local head loss

There are pipe fittings such as bend pipes and reducing joints in the equipment. These pipe fittings are short, so we assume that the local frictional pressure drop accounts for approximately 10% of the sum of the three-segment frictional pressure drop.

$$h_{2-3} + h_{4-5} = (h_{1-2} + h_{3-4} + h_{5-6}) \times 10\% \tag{25}$$

5.6. Calculations and analysis of results

As shown in Fig. 13, when PVC pipes with low roughness are used at temperatures from 0–30 °C, the ratio of the frictional head loss caused by sidewall friction is approximately 0.02 % – 0.12 %. The change in temperature does not practically affect the sidewall friction effect.

When pipes with higher roughness are used, such as reinforced-concrete pipes, the ratio of the frictional head loss caused by the

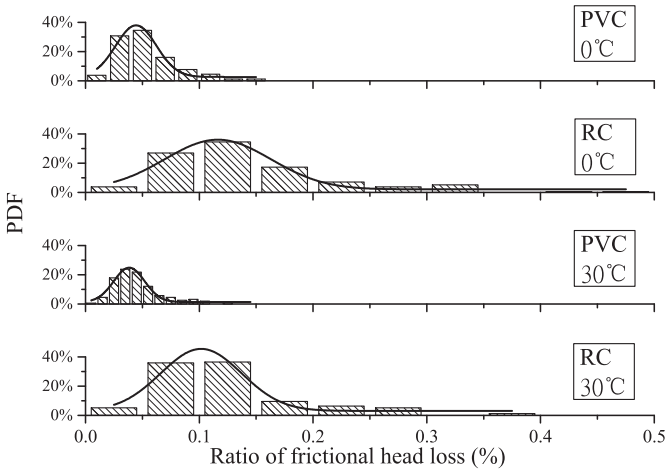

Fig. 13. Comparison of the fitted distributions (solid lines) and experimental observations (histograms) for different temperatures and materials. PDF is the abbreviation for probability density function.

sidewall friction is approximately 0.05 % – 0.35 % (Fig. 13). Compared to the condition of using PVC, the roughness change affects the sidewall friction effect.

Regardless of the materials used in the projects, the roughness is typically between the conditions of PVC pipes and reinforced concrete pipes ($n = 0.017$) based in Table 3. Thus, the ratio of the frictional head loss caused by the sidewall friction is always less than 0.5 %, which is the maximum on the horizontal axis in Fig. 13. The value of 0.5 % in both cases is so small from the engineering viewpoint that the frictional head loss caused by sidewall friction can be neglected.

6. Conclusions

Considering the problem of the under-utilization of low-head water power because of its inefficiency, a less intrusive and more efficient solution is proposed: the Low Water-Head Hydropower Project, which is an automatic pump that can transmute low-water-head hydropower into high-pressure gas power and is highly efficient. In this paper, we study the first part, the Gas-Water Energy Conversion Equipment. The goal of our study is to improve the energy conversion efficiency from low-head water to high-pressure gas. The energy transfer process from water to air has not been examined in previous studies. Based on the methods in two-phase flow studies to detect a pressure drop, a new method is proposed to estimate the energy loss of different forms generated by low-head water, focusing on the vertical downflow where the gas and liquid dramatically mix together. Energy balance equations based on the one-dimensional homogeneous model from the Bernoulli equation were established. Through the energy balance equations, the percentages of different forms of energy loss were determined. According to the statistical analysis of the test data, the energy conversion efficiency is 14–44%.

Wider and higher outlet pipes had higher η. Engineers can follow the table we introduced to determine the d' based on the specific flow rate and river drops in their project. But because the outlet pipe is buried underground in engineering and if the outlet pipe is higher, it will be buried deeper and the costs will increase. Thus, the selected h' must be carefully determined before use in engineering applications. The ratio of the frictional head loss caused by the sidewall friction is always less than 0.5 %. From an engineering viewpoint, the value of 0.5 % in both cases is so small that the frictional head loss caused by the sidewall friction can be neglected. In addition, the change in temperature does not practically affect the sidewall friction effect.

The high-pressure gas power generated by this device does not require connection to the grid and can be directly utilized. Therefore, the system can avoid energy loss during long transport. Currently, this system is only for water-scarce mountainous regions in Yunnan Province to pump water from the foot of the mountains to the hillsides. Further research could explore other ways of utilizing high-pressure gas and transforming high pressure gas power into other forms of available energy.

Acknowledgments

This research was funded by the National Natural Science Foundation of China (NSFC, Grant Numbers 41672257 & 51309151) and by the Opening Project of the State Key Laboratory of Hydrology-water Resources and Hydraulic Engineering, Nanjing Hydraulic Research Institute (Project Number: 2016491611). Their financial support is gratefully acknowledged.

References

[1] C. Wang, J. Li, Construction and application of water quantity evaluation system for yunnan water resources bulletin, Hydrography (in Chin.) 37 (2017) 75–80.
[2] Y. Liu, L. Tan, Tip clearance on pressure fluctuation intensity and vortex characteristic of a mixed flow pump as turbine at pump mode, Renew. Energy 129 (2018) 606–615.
[3] Y. Hao, L. Tan, Symmetrical and unsymmetrical tip clearances on cavitation performance and radial force of a mixed flow pump as turbine at pump mode, Renew. Energy 127 (2018) 368–376.
[4] B.S. Thapa, O.G. Dahlhaug, B. Thapa, Sediment erosion induced leakage flow from guide vane clearance gap in a low specific speed francis turbine, Renew. Energy 107 (2017) 253–261.
[5] O. Francois, T.J. Gilmore, M.J. Pinto, S.M. Gorelick, A physically based model for air-lift pumping, Water Resour. Res. 32 (1996) 2383–2399.
[6] R.R. Mankbadi, S. Mikhail, A turbine-pump system for low-head hydropower, Energy Convers. Manag. 25 (1985) 339–344.
[7] A. Date, A. Date, A. Akbarzadeh, Performance investigation of a simple reaction water turbine for power generation from low head micro hydro resources, Smart Grid Renew. Energy 03 (2012) 239–245.
[8] A.G. Parygin, A.V. Volkov, A.V. Ryzhenkov, Commentary on the efficiency of selected structural designs of low head micro hydraulic power plants, Math. Model Methods Appl. Sci. 9 (2015) 116.
[9] A. Roberts, B. Thomas, P. Sewell, P. Hoare, Generating Renewable Power from Water Hammer Pressure Surges, Renew. Energy 134 (2019) 1392–1399.
[10] F.A. Zenz, Explore the potential of air-lift pumps and multiphase, Chem. Eng. Prog. 89 (1993) 51–56.
[11] H. Gvirtzman, S.M. Gorelick, Using air-lift pumping as an in-situ aquifer remediation technique, Water Sci. Technol. 27 (1993) 195–201.
[12] S. Guet, G. Ooms, Fluid mechanical aspects of the gas-lift technique, Annu. Rev. Fluid Mech. 38 (2006) 225–249.
[13] R.W. Lockhart, R.C. Martinelli, Proposed correlation of data for isothermal two-phase, two-component flow in pipes, Chem. Eng. Prog. 45 (1949) 39–48.
[14] A.E. Dukler, M. Wicks, R.G. Cleveland, Frictional pressure drop in two phase flow: B. an approach through similarity analysis, AIChE J. 10 (1964) 44–51.
[15] D.R.H. Beattie, P.B. Whalley, A simple two-phase frictional pressure drop calculation method, Int. J. Multiphas. Flow 8 (1982) 83–87.
[16] H. Mullersteinhagen, K. Heck, A simple friction pressure drop correlation for two-phase flow in pipes, Chem. Eng. Process 20 (1986) 297–308.
[17] K.A. Triplett, S.M. Ghiaasiaan, S.I. Abdelkhalik, D.L. Sadowski, Gasliquid two-phase flow in microchannels part i: two-phase flow patterns, Int. J. Multiphas. Flow 25 (1999) 377–394.
[18] T. Sawai, M. Kaji, T. Kasugai, H. Nakashima, T. Mori, Gasliquid interfacial structure and pressure drop characteristics of churn flow, Exp. Therm. Fluid Sci. 28 (2004) 597–606.
[19] B.A. Shannak, Frictional pressure drop of gas liquid two-phase flow in pipes, Nucl. Eng. Des. 238 (2008) 3277–3284.
[20] T. Zhao, Q. Bi, Pressure drop characteristics of gas-liquid two-phase flow in vertical miniature triangular channels, Int. J. Heat Mass Tran. 44 (2001) 2523–2534.
[21] K. Nilpueng, S. Wongwises, Flow pattern and pressure drop of vertical upward gas-liquid flow in sinusoidal wavy channels, Exp. Therm. Fluid Sci. 30 (2006) 523–534.
[22] T. Fukano, A. Kariyasaki, Characteristics of gas-liquid two-phase flow in a capillary tube, Nucl. Eng. Des. 141 (1993) 59–68.
[23] S. Wang, J. Huang, K. He, J. Chen, Phase split of nitrogen/non-Newtonian fluid two-phase flow at a micro-t-junction, Int. J. Multiphas. Flow 37 (2011) 1129–1134.
[24] F. Liang, H. Zheng, Y. Sun, L. Song, Experimental investigation of phase split of gasliquid two-phase flow through small holes at the pipe wall, Exp. Therm. Fluid Sci. 76 (2016) 330–341.
[25] P. Zhao, L. Gao, J. Wang, Y. Dai, Energy efficiency analysis and off-design analysis of two different discharge modes for compressed air energy storage system using axial turbines, Renew. Energy 85 (2016) 1164–1177.
[26] D. Li, Y. Xuan, E. Yin, Q. Li, Conversion efficiency gain for concentrated triple-junction solar cell system through thermal management, Renew. Energy 126 (2018) 960–968.
[27] D. Chisholm, Pressure gradients due to friction during the flow of evaporating two-phase mixtures in smooth tubes and channels, Int. J. Heat Mass Tran. 16 (1973) 347–358.